Simultaneously measuring image features and resolution in live-cell STED images

Andrew E. S. Barentine[1,2], Lena K. Schroeder[1], Michael Graff[1], David Baddeley[*,1,3], and Joerg Bewersdorf[*,1,2]

[1]Department of Cell Biology, Yale University School of Medicine, PO Box 208002, New Haven, Connecticut 06520-8002 USA.
[2]Department of Biomedical Engineering, Yale University, PO Box 208267, New Haven, Connecticut 06520-826
[3]Auckland Bioengineering Institute, University of Auckland, Private Bag 92019, Auckland 1142, New Zealand
[*]Corresponding authors

September 19, 2017

Abstract

Reliable interpretation and quantification of cellular features in fluorescence microscopy requires an accurate estimate of microscope resolution. This is typically obtained by measuring the image of a non-biological proxy for a point-like object, such as a fluorescent bead. While appropriate for confocal microscopy, bead-based measurements are problematic for Stimulated Emission Depletion (STED) and similar techniques where the resolution depends critically on the choice of fluorophore and acquisition parameters. We demonstrate that for a known geometry, e.g. tubules, the resolution can be accurately measured by fitting a model that accounts for both the Point Spread Function (PSF) and the fluorophore distribution. To address the problem of coupling between tubule diameter and PSF width, we developed a technique, Nested-loop Ensemble PSF (NEP) fitting. NEP fitting enables extraction of the size of cellular features and the PSF in fixed-cell and live-cell images without relying on beads or pre-calibration. We validate our technique using fixed microtubules and apply it to measure the diameter of endoplasmic reticulum tubules in live COS-7 cells. NEP fitting has been implemented as a plugin for the PYthon Microscopy Environment (PYME), a freely available and open source software.

Introduction

All fluorescence microscopy images distort the underlying object, failing to capture details smaller than a certain size. These distortions are described by the system's Point-Spread Function (PSF), and knowledge of this PSF is essential when interpreting the images produced and in ensuring that quantitative measurements are accurate. For many purposes it is sufficient to summarize the effects of the PSF in a simple resolution figure, e.g. the full-width at half maximum (FWHM). A popular method for obtaining the PSF FWHM is extracting an intensity line profile from a fluorescent bead image and either directly measuring the FWHM or estimating it more accurately by fitting a Gaussian or Lorentzian (in the case of STED) model to the profile. For diffraction-limited microscopes, beads can be regarded as point-sources because they are significantly smaller than the FWHM of the PSF (typically 20-100 nm and 250 nm, respectively) and the fit FWHM is taken to be that of the PSF.

When considering STED microscopy, where the PSF FWHM is on the order of 50 nm, the assumption that the PSF is much larger than the bead size is no longer valid, as beads whose size is similar to that of the PSF are often needed to achieve reasonable signal levels. The resolution in STED microscopy is also strongly affected by the excitation and depletion cross-sections of the dye chosen, the choice of laser powers,

and the effect of both dye micro-environment and (comparatively minor) sample-induced aberrations in the depletion beam, making beads a particularly poor proxy for the true resolution achieved when imaging cellular samples.

Measuring STED resolution on a target within the same cellular environment, labelled with the same dye(s) and imaged with the same choice of laser powers avoids most of these issues. Microtubules labelled with the same fluorescent dye as the final target structure are an attractive candidate which can be readily prepared. The simplest and most common labelling protocol that usually results in bright stainings is indirect immunofluorescence. Labeling the 25 nm outer diameter of a microtubule with primary and secondary antibodies results in a structure that is 60 nm in diameter as observed using electron microscopy [1]. This is within the size range of the PSF and therefore, as with beads, the thickness of the structure is non-negligible when quantifying the resolution in a STED microscope.

To determine the impact this finite object size has on resolution quantification using the popular Gaussian- and Lorentzian-fitting techniques, we simulated intensity line profiles perpendicular to the long axis of antibody-labeled microtubules imaged at various resolutions, and fit them with Gaussian and Lorentzian functions.

To simulate the intensity profiles, we modeled the PSF as a Lorentzian, a common STED PSF approximation [2], and modeled the fluorophore distribution for the primary and secondary antibody labeled microtubule as an annulus of 25 nm inner diameter and 60 nm outer diameter, as measured for densely-labeled microtubules [1] (top of 1A). For most STED microscopes, the axial (z) PSF FWHM is considerably larger (500-700 nm) than the FWHM along the lateral (xy) directions. This means that the entire cross-section of a microtubule is effectively summed along the axial dimension during imaging, as shown by the red curve in figure 1A. The imaging process is simulated by convolving the fluorophore distribution with the PSF model (red curve and black curve, respectively, in fig. 1A). The resulting line profile cross section of a microtubule imaged with a 50 nm FWHM PSF is shown in figure 1A (green curve).

We simulated line profiles across microtubules imaged with STED resolutions ranging from 20 to 100 nm (PSF FWHM) and shot noise added, and fit them with simple Lorentzian and Gaussian functions. The FWHM of the Lorentzian fits were substantially larger than the PSF FWHM they were simulated with, and this effect was even more pronounced for the fitted Gaussian FWHM (fig. 1B), confirming that simple fitting of these models does not result in an accurate resolution figure. Similar Gaussian or Lorentzian fits in which the width is interpreted as the size of an imaged structure rather than resolution are popular in various types of fluorescence (super-resolution) microscopy. Interpreting Figure 1B this way, shows that this approach only yields reasonable results when the PSF is much smaller (>3x) than the imaged structure. When used to quantify resolution, the inaccuracy increases, as expected, at higher resolutions (smaller PSF FWHM), making it particularly problematic for STED microscopy, where relative errors of 100% can easily occur. We conclude that using the FWHM of Gaussian or Lorentzian fits is an inaccurate measure for both resolution and feature size quantification.

In order to accurately determine microscope resolution or feature size from line profile cross-sections, both the microscope PSF and the geometric distribution of fluorophores on the labeled structure must be modeled in the function used for fitting. Previous efforts have fixed one of these parameters - assuming that either the PSF, or the structure size is already known [3], or qualified the FWHM based on simulations using a known PSF or structure size [4]. These approaches are, however, limited in that in biological STED microscopy both structure size and resolution are typically unknown. Fitting both of these parameters simultaneously, on the other hand, is difficult as they are not strictly independent. Increases in either parameter give rise to an increased profile width, albeit with subtly different effects on profile shape. At the signal-to-noise level typical of a single profile it is difficult to separate the effects of the two parameters. This coupling can result in inaccurate estimates for both values. Here, we present a tool which overcomes this challenge, and allows simultaneous fitting of structure size and PSF width.

Ensemble PSF Fitting

Treating both the PSF width and the structure size as free parameters, it should, in principle, be possible to determine both simultaneously. To make the fit more robust, we fit multiple profiles and exploit the prior that the PSF width should be the same for each profile. We accomplish this by performing a two-layer nested

fit, such that in the inner fit, all tubules are fit with the PSF FWHM constrained to be the same value, Γ, and the mean squared error (MSE) for each tubule is reported. The outer fit is then responsible for finding the value of Γ which minimizes the mean MSE taken over all of the tubule fits, which has a propensity to be well-behaved and smooth over values near the expected PSF FWHM (fig. 1C). This technique, which we refer to as nested-loop ensemble PSF (NEP) fitting, constrains the fit enough that more accurate PSF widths and microtubule diameters can be determined, as shown in figure 1B, D.

NEP fitting using the antibody-coated tubule model yielded significantly better results than fitting with plain Gaussian or Lorentzian functions, and the PSF widths calculated by the fit are in close agreement with the ground truth (fig. 1B). Notably, NEP fitting with the antibody-coated tubule model simultaneously yields accurate measures of the simulated microtubule diameter, 25 nm, for all simulated PSFs with FWHM equal to or less than 60 nm, which is the point at which the PSF FWHM becomes larger than the outer diameter of the antibody coat (fig. 1D). For structures whose size does not vary in a cell, e.g. microtubule diameters, the structure size can additionally be constrained as an ensemble parameter during the fit, although we did not find this to be a necessary step.

Software and Validation

We implemented NEP fitting for STED images of surface-labeled or label-filled tubules in the PYthon Microscopy Environment (PYME). Line profiles of a user-defined thickness are extracted from images loaded into PYME, after which they can be fit using a variety of model functions. Alternatively, they can be saved/appended to several file formats (HDF, json) for later analysis or ensemble fitting with profiles from multiple images. The line profile extraction GUI is shown in figure 2A.

STED PSF size is dependent on the STED laser power with a scaling of $\frac{\alpha}{\sqrt{1+I/I_s}}$ [5]. To test the efficacy of ensemble fitting on real data, we imaged primary and secondary antibody labeled microtubules using a Leica SP8 STED 3X microscope with different STED laser powers. After extracting 239 line profiles from a total of 28 images (example shown in fig. 2B, n=74, n=71, and n=94 profiles extracted from N=8, N=8, and N=12 images of N=3, N=3, and N=6 cells, acquired at 27.7, 55.6, and 110.6 mW STED laser powers, respectively), NEP fitting was performed. As shown in figure 2C, this demonstrates that our fit is responsive to changes in PSF size resulting from varied STED laser powers, and can reproduce the expected scaling of the PSF widths with the STED laser power.

To determine if our ensemble (NEP) fitting approach in which the PSF width is constrained to a single, global value for all profiles is beneficial, we compared its results with those obtained when both PSF width and tubule diameter were optimized on a per-profile basis. We performed this comparison on images recorded with 110.6 mW depletion power. While fits performed without an ensemble PSF have more degrees of freedom and therefore usually yield smaller residuals, they often come at the expense of accuracy in the measured values. This can be seen in figure 2D, where the standard least squares fit results in an average microtubule diameter of 30 $\pm$ 13 nm (mean $\pm$ SD), compared to the NEP-fitted value of 28 $\pm$ 8 nm (mean $\pm$ SD), and the expected value of 25 nm. NEP fitting, with its global PSF constraint, indeed improves the measurement of the microtubule diameter, as evidenced by the reduced spread in tubule diameters and average value closer to the expected 25 nm. The PSF FWHM of standard least squares fitting was 45 $\pm$ 10 nm (mean $\pm$ SD), compared to the NEP-fitted value of 44 nm. We note that fitting a single line profile would not provide a reliable measure of either PSF FWHM or tubule diameter, and could lead to relative errors of 100% for both values. The minimum number of profiles necessary for robust NEP fitting depends on the fluorophore distribution and the relative PSF size. However, even for cases of low signal-to-noise ratio (SNR), we found 100 profiles to be sufficient for the fluorophore distributions tested (see fig. S1, S2).

Application to live-cell images

While the robust PSF measurement in fixed cells by NEP fitting is a substantial improvement over bead calibrations, a large advantage of NEP fitting is that it can be performed on live-cell data for in-situ resolution calibration in the most biologically relevant state. We applied ensemble PSF fitting in live-cell STED images of label-filled or surface-labeled endoplasmic reticulum (ER) tubules, using ss-SNAP-KDEL or SNAP-Sec61β,

respectively (fig. 3A-D). In order to fit the label-filled tubules, we modeled the fluorophore distribution perpendicular to the long axis of the tubule as a filled circle, which projects as $2\sqrt{R^2 - x^2}$, where R is the radius, which we then convolved with a Lorentzian to account for the imaging process, as before. We modeled the fluorophore distribution for surface-labeled tubules as an annulus, like the microtubules, only with a much smaller thickness than an antibody coat, as SNAP-tag [6] is about 4 nm in diameter, and the organic dye itself can be estimated to have a radius of 0.5 nm assuming they are both globular [7], resulting in a 4.5 nm thick annulus. Fits of ER tubule diameter for various test PSF widths show stronger coupling between the tubule diameter and PSF width for label-filled tubules than surface-labeled tubules (fig. 3E,F). The PSF widths from the NEP fit were 45.8 nm for the label-filled profiles, and 43.7 nm for the surface-labeled profiles, FWHM (fig. 3G,H).

Notably, the standard deviation for both the label-filled and surface-labeled tubule diameters is fairly large: 30 and 15 nm, respectively (with mean values of 132 nm and 101 nm). To test whether this variability in tubule diameter is primarily biological in nature, or dominated by the SNR-limited fit precision, we simulated tubule profiles of known diameter with similar signal-to-noise ratios, convolved with 50 nm FWHM Lorentzians. The distributions of fitted diameters were more narrow than those observed in the live-cell images, with standard deviations of only 5 nm for the membrane-labeled tubules, and 12 nm for the label-filled tubules (fig. S1). The larger range of label-filled tubule fitted diameters is expected because the fluorophore distribution orthogonal to the long axis of the tubule looks more similar to the PSF than a surface-labeled fluorophore distribution. This is reflected in the live-cell data, where the tubule diameter is more strongly coupled to the PSF width for the label-filled tubules, as shown in the heat-maps of tubule diameter histograms when fit with various fixed PSF widths (Figures 3E,F). We therefore expect roughly half of the spread in tubule diameter to be biological in origin. Notably, the NEP fitting estimates for tubule diameter and PSF width do not suffer from systematic errors when the signal-to-noise ratio (SNR) of the profile is decreased. However, the variability in fit tubule diameters for individual profiles is increased for lower SNR profiles (fig. S2).

Discussion

Traditional methods of resolution calibration in STED microscopy are problematic for biological quantification. The NEP fitting method introduced in this paper addresses this issue and provides a robust and practical means to both quantify the performance of a microscope, as well as improve feature measurements within the image. Its implementation in a freely-downloadable, open source, cross-platform software package allows for rapid adoption by others, without requiring mathematical or programming expertise. The principle of ensemble fitting can be readily extended to other fluorescence microscopy modalities, e.g. confocal, by substituting a different functional representation of the PSF when producing the model function for fitting; the only requirement is that the labeling geometry of the structure be known. This known geometry is not limited to tubules, and can be extended to fit objects like beads or vesicles, which would be useful for cell-trafficking studies. The accurate measure of PSF width afforded by NEP fitting can be used to quantify microscope performance under various conditions, refine models of organelle morphology, and remove uncertainty in parameter selection for deconvolution or other image enhancement algorithms.

Software Availability

All line profiles were drawn, extracted, and fit using the open source PYthon Microscopy Environment (PYME) and the NEP Fitting plug-in, which are both freely available [8, 9].

Acknowledgements

This work is supported in part by NIH grant S10 OD020142 for imaging resources (for the Leica TCS SP8 STED 3X microscope), the G. Harold & Leila Y. Mathers Foundation, the Wellcome Trust (095927/A/11/Z, 203285/B/16/Z), and the Yale Diabetes Research Center (NIH P30 DK045735). A. E. S. B. acknowledges support by an NIH training grant (T32 GM008283). J. B. discloses significant financial interest in Bruker Corp. and Hamamatsu Photonics. We thank Phylicia Kidd and Mark Lessard for providing biological test samples.

References

[1] K Weber, P C Rathke, and M Osborn. Cytoplasmic microtubular images in glutaraldehyde-fixed tissue culture cells by electron microscopy and by immunofluorescence microscopy. *Proceedings of the National Academy of Sciences of the United States of America*, 75(4):1820–4, 1978.

[2] Francesca Bottanelli, Emil B Kromann, Edward S Allgeyer, Roman S Erdmann, Stephanie Wood Baguley, George Sirinakis, Alanna Schepartz, David Baddeley, Derek K Toomre, James E Rothman, and Joerg Bewersdorf. Two-colour live-cell nanoscale imaging of intracellular targets. *Nature communications*, 7(May 2015):10778, 2016.

[3] D. Baddeley, Y. Weiland, C. Batram, U. Birk, and C. Cremer. Model based precision structural measurements on barely resolved objects. *Journal of Microscopy*, 237(1):70–78, 2010.

[4] Lars Meyer, Dominik Wildanger, Rebecca Medda, Annedore Punge, Silvio O. Rizzoli, Gerald Donnert, and Stefan W. Hell. Dual-color STED microscopy at 30-nm focal-plane resolution. *Small*, 4(8):1095–1100, 2008.

[5] Stefan W Hell. Far-Field Optical Nanoscopy. *Science*, 316(5828):1153–1158, 2007.

[6] Antje Keppler, Susanne Gendreizig, Thomas Gronemeyer, Horst Pick, Horst Vogel, and Kai Johnsson. A general method for the covalent labeling of fusion proteins with small molecules in vivo. *Nature Biotechnology*, 21(1):86–89, 2002.

[7] Harold P. Erickson. Size and shape of protein molecules at the nanometer level determined by sedimentation, gel filtration, and electron microscopy. *Biological Procedures Online*, 11(1):32–51, 2009.

[8] David Baddeley. Python Microscopy Environment. python-microscopy.org.

[9] Andrew E. S. Barentine, Michael Graff, and David Baddeley. Code repository: Nested-Loop Ensemble Fitting. bitbucket.org/david_baddeley/nep-fitting.

[10] Fang Huang, George Sirinakis, Edward S. Allgeyer, Lena K. Schroeder, Whitney C. Duim, Emil B. Kromann, Thomy Phan, Felix E. Rivera-Molina, Jordan R. Myers, Irnov Irnov, Mark Lessard, Yongdeng Zhang, Mary Ann Handel, Christine Jacobs-Wagner, C. Patrick Lusk, James E. Rothman, Derek Toomre, Martin J. Booth, and Joerg Bewersdorf. Ultra-High Resolution 3D Imaging of Whole Cells Resource Ultra-High Resolution 3D Imaging of Whole Cells. *Cell*, 166(4):1028–1040.

[11] Lena K. Schroeder, Andrew E. S. Barentine, Sarah Schweighofer, David Baddeley, Joerg Bewersdorf, and Shirin Bahmanyar. Nano-scale sized holes in ER sheets provide an alternative to tubules for highly-curved membranes. *Submitted*.

Materials and Methods

Tubule Model Functions

The model functions used in ensemble PSF fitting were derived by taking the projection of the fluorescence labeling geometry onto the xy-plane and then convolving this projection with a model of the microscope PSF, in this work a Lorentzian. Derivation of the functions used was carried out in Mathematica.

Principle

Inherent in the imaging process is the convolution of the Point-Spread Function (PSF) with the structure being imaged.

$$I(x,y,z) = h(x,y,z) \otimes s(x,y,z) \tag{1}$$

where I is the resulting image, h is the PSF, and s is the fluorophore distribution. We only consider tubule cross sections because the profile of the tubule is uniform along its long-axis (y), and can therefore write the convolution as

$$C(x,z) = \int_{-\infty}^{\infty}\int_{-\infty}^{\infty} h(\tau_1,\tau_2)s(x-\tau_1, z-\tau_2)d\tau_1 d\tau_2, \tag{2}$$

where C is the cross section of the 3D image of the tubule.

For standard STED microscopy, the full-width at half-maximum (FWHM) of the PSF along the axial dimension is significantly larger than the tubular structures we consider, such that the convolution along the axial dimension reduces to a sum. We can now write

$$P(x) = \int_{-\infty}^{\infty} h(t)p(x-t)dt, \tag{3}$$

where P is the line profile cross section, p is the projection of s (summed over z), and h is the 1D lateral profile of the PSF.

Annulus fluorophore distribution

The cross section of a surface-labeled tubule can be taken to be an annulus, where we assume that the fluorophores are uniformly distributed between the inner and the outer radius. Again, due to the large axial FWHM of the STED PSF, the convolution along the axial dimension reduces to a sum. We calculate this sum by considering half of an annulus, and subtracting the z position of the inner radius edge, $z_i(x)$, from the outer radius edge, $z_o(x)$,

$$z_i(x) = \left(H\left(x+r\right) - H\left(x-r\right)\right) r\sin\left(\theta_i\right), \tag{4}$$

and

$$z_o(x) = \left(H\left(x+R\right) - H\left(x-R\right)\right) R\sin\left(\theta_o\right), \tag{5}$$

respectively, where H is the Heaviside step function, R is the outer radius of the annulus, r is the inner radius, $\theta_o = \arccos\left(\frac{x}{R}\right)$, and $\theta_i = \arccos\left(\frac{x}{r}\right)$. We can now write the projection of the annulus simply as

$$p_{\text{annulus}}(x) = \frac{2\left(z_o(x) - z_i(x)\right)}{\pi\left(R^2 - r^2\right)}, \tag{6}$$

where the factor of two accounts for the top and bottom halves of the annulus, and we have sum-normalized $p_{\text{annulus}}(x)$.

The Lorentzian function in 1D is given by

$$L(x) = \frac{1}{2\pi}\frac{\Gamma}{x^2 + \left(\frac{\Gamma}{2}\right)^2}, \tag{7}$$

where Γ is the FWHM. Substituting $L(x)$ for the 1D PSF, we can determine the line profile intensity of an annulus structure imaged with a Lorentzian PSF:

$$P_{\text{annulus}}(x) = \int_{-\infty}^{\infty} L(t)p_{\text{annulus}}(x-t)dt, \tag{8}$$

$$\begin{aligned} &= \alpha\Bigg[\Gamma\left(\sqrt{1+\frac{4r^2}{(\Gamma-2ix)^2}} + \sqrt{1+\frac{4r^2}{(\Gamma+2ix)^2}} - \sqrt{1+\frac{4R^2}{(\Gamma-2ix)^2}} - \sqrt{1+\frac{4R^2}{(\Gamma+2ix)^2}}\right) \\ &\quad + 2ix\left(-\sqrt{1+\frac{4r^2}{(\Gamma-2ix)^2}} + \sqrt{1+\frac{4r^2}{(\Gamma+2ix)^2}} + \sqrt{1+\frac{4R^2}{(\Gamma-2ix)^2}} - \sqrt{1+\frac{4R^2}{(\Gamma+2ix)^2}}\right)\Bigg], \end{aligned} \tag{9}$$

where $\alpha = \frac{1}{2\pi(r-R)(r+R)}$.

Label-filled Model Function

In order to derive a label-filled model function, which can be used to model a lumen-labeled ER tubule, we have two options. The first approach would be to follow the same steps as above using the projection of a circle, which is a semi-circle

$$p_{\text{circle}}(x) = \frac{2\sqrt{R^2 - x^2}}{\pi R^2}, \tag{10}$$

where R is the radius and we have sum-normalized. However, we can also simply set the inner radius of the annulus model function to zero, which yields

$$P_{\text{circle}}(x) = \int_{-\infty}^{\infty} L(t) p_{\text{circle}}(x-t)dt \tag{11}$$

$$= P_{\text{annulus}}(x)\Big|_{r=0} \tag{12}$$

$$= -\frac{\Gamma\left(-\sqrt{1+\frac{4R^2}{(\Gamma-2ix)^2}} - \sqrt{1+\frac{4R^2}{(\Gamma+2ix)^2}} + 2\right) + 2ix\left(\sqrt{1+\frac{4R^2}{(\Gamma-2ix)^2}} - \sqrt{1+\frac{4R^2}{(\Gamma+2ix)^2}}\right)}{2\pi R^2} \tag{13}$$

Deriving new model functions

Similar model functions can be derived for other target structures, with the caveat that they might not be as simple as the tubule models above. Tubules and other linear structures represent an easy class of structure to model because the cross-section is relatively uniform along the long-axis of the tubule, allowing the convolution to be ignored along that direction, and the model function to be generated only considering a single dimension. Other geometries do not allow this reduction in dimensionality, and the convolution integrals must be performed in 2 or 3D. This makes analytic model functions for STED microscopy, in particular, difficult, as 2D Lorentzians cannot be analytically normalized. In the absence of a closed analytic form, NEP fitting can be performed using numeric model functions albeit with significantly poorer computational speed.

Microtubule Simulations

Microtubule line profiles were simulated using a Lorentzian-convolved annulus model function, where the annulus had an inner diameter of 25 nm and outer diameter of 60 nm to account for a dense primary- and secondary-antibody coat [1]. The center position of each microtubule was randomly varied at the sub-pixel level to avoid aliasing, and the values generated from the model were then used as expectation values in generating and sampling Poisson distributions to add shot noise to the model. The amplitude and background levels were chosen such that the signal-to-noise ratio is comparable to our fixed-cell microtubule images. The FWHM of the Lorentzian-shaped PSF was varied between 20 and 100 nm, and 50 microtubule line profiles were simulated with each PSF width.

ER Tubule Simulations

ER tubule line profiles were simulated using both label-filled and surface-labeled tubule model functions, where the model function describes the expected shape of a line profile drawn perpendicular to the long axis of a straight region of tubule. The fluorophore distribution for the surface label was taken to be an annulus of 115 nm inner diameter projected onto a line, with outer diameter 124 nm, where the 4.5 nm thickness is to account for the SNAP-tag and organic dye molecule, which were both assumed to be globular in estimating their diameters [7]. The label-filled fluorophore distribution was modeled as a circle of 115 nm diameter projected onto a line. The fluorophore distributions for each model were convolved with a Lorentzian of 50 nm FWHM to emulate the microscope resolution. First, 100 profiles of each model were simulated, with their center positions randomly varied at the sub-pixel level to avoid aliasing. The intensity values generated by each model were used as expected values in generating and sampling Poisson distributions to add shot noise levels comparable to the ss-SNAP-KDEL and SNAP-sec61β live-cell images contained in this work. Ensemble fitting was then performed on the tubules corresponding to each model, and the fitted diameters

were plotted in histograms (fig. S1). Second, we simulated profiles at various signal-to-noise levels. The profiles were generated in the same way, except that the pre-shot-noise background was varied from 0 to 300, while the amplitude was kept constant at 100. Due to the nature of Poisson statistics, this generates tubules with substantially different noise levels. One hundred line profiles were simulated at each noise level.

Fitting

Fitting was performed in PYME using the Scipy package, specifically the Levenberg-Marquardt and Nelder-Mead minimization algorithms. For standard, non-NEP fitting, profile fits were performed with the Scipy package Levenberg-Marquardt implementation. All initial parameter guesses were automatically estimated. The background (offset from zero) was estimated to be the minimum intensity value of the profile, the amplitude of the profile was estimated to be the maximum intensity value minus the background, and the center position was estimated to be the position of the maximum intensity value. The FWHM of the Gaussian and Lorentzian functions, and the tubule diameter and PSF FWHM of the Lorentzian-convolved model functions were all estimated to be the FWHM of the profile, which was determined by counting the number of pixels with intensity values above the background plus half of the amplitude.

For NEP fitting, which was only applied using the Lorentzian-convolved model functions, the inner loop fitting was performed similarly to the standard fitting, with the only difference being that the inner loop did not try to optimize the PSF FWHM, and instead took this value as an input parameter parsed by the outer loop. The inner loop returned the mean of the mean squared errors (mean MSE) taken over each of the individual tubules fits, and this value was minimized in the outer loop fit using a Nelder-Mead minimization, where the only parameter directly controlled by the Nelder-Mead minimization was the PSF FWHM. In order to estimate the uncertainty of the PSF FWHM fit, the result from the Nelder-Mead minimization was passed as an initial guess to a Levenberg-Marquardt minimization to approximate the variance of the estimate. We used the Nelder-Mead algorithm for the primary parameter estimation because we found it to converge faster. In order to facilitate the estimation of the variance, the inner loop passed the Levenberg-Marquardt minimization an array of the residuals appended from each of the tubule profile fits. The variance estimate is calculated by multiplying the residual variance by the jacobian about the fit result.The standard deviation, however, is often below 1 nm for NEP fitting, which we take to be an underestimate of the uncertainty in the measurement.

Cell Culture

COS-7 (ATCC, CRL-1651) cells were grown in a standard mammalian cell incubator with 5% CO2 environment using phenol red free DMEM (Thermo Fisher Gibco) or DMEM/F-12 (Thermo Fisher Gibco) media supplemented with 10% FBS (Thermo Fisher Gibco). Cells were transfected by electroporation using a Super Electroporator NEPA21 Type II (Nepa Gene). Electroporation cuvettes with a 2 mm gap were loaded with 10^6 cells suspended in Opti-MEM (Thermo Fisher Gibco) and 2.5-10 µg DNA, depending on the desired expression level. Transfected cells were imaged 12-48 hours after electroporation.

Microtubule Samples

Microtubule samples were prepared using the method described by Huang et al (2016) [10]. Briefly, COS-7 cells were grown on coverglass and pre-extracted using saponin before fixation with 3% paraformaldehyde + 0.1% glutaraldehyde. Mouse anti-α-tubulin antibody (Sigma-Aldrich, T5168) was used to label microtubules. A goat anti-Mouse labeled with Atto647N (Sigma-Aldrich) was used as a secondary antibody. Samples were mounted in Prolong Diamond Antifade Mountant (Thermo Fisher Scientific) and imaged at room temperature.

ER Samples

The SNAP-Sec61β images used are a subset of images from a broader study on ER morphology [11]. COS-7 cells were electroporated with either SNAP-Sec61β [2] or ss-SNAP-KDEL and plated in glass-bottom dishes (MatTek, 35 mm, no. 1.5). SNAP tagged proteins were labeled immediately before imaging with 1 µM

SiR-BG (New England Biolabs, S9102S) according to manufacturer's instructions. Living cells were imaged with 5% CO2, in Live Cell Imaging Solution (Thermo Fisher Scientific), and at 37 C using a stage incubator and objective heater.

STED Microscopy

Images were acquired using a Leica SP8 STED 3X equipped with a Onefive Katana-08HP pulsed laser as a STED source and a SuperK Extreme EXW-12 (NLT Photonics) pulsed white light laser as an excitation source. All images were acquired using a HC PL APO 100x 1.40 NA Oil CS2 objective. Living cells were scanned with 8000 Hz at 37 C with 5% CO2. Fixed cells were scanned with 1000 Hz at room temperature. Images were acquired using 16 line averages. All samples were imaged with 633 nm excitation and 775 nm STED wavelengths, with STED power at 110.6 mW for all images of ER. Emission light between 650-750 nm was collected using gating, set to 0.3-6 ns, on a HyD hybrid detector. The pinhole was set to 1 Airy unit.

Depletion Power Measurements

STED laser powers on the Leica SP8 STED 3X were measured using a microscope slide power meter sensor head (ThorLabs, S170C) with a digital handheld optical power meter console (ThorLabs, PM100D). A Onefive Katana-08HP pulsed laser was used as a STED source. Laser power at 775 nm wavelength was measured using settings to slowly scan a very small region with minimal beam blanking, which allowed us to detect the STED laser as a point rather than a scanned line. A 8192 x 8192 pixel region was scanned with 10 Hz scan speed, with zoom set at maximum of 48, and using bidirectional scanning at room temperature. These settings effectively scanned a 2.42 x 2.42 µm region with 295.68 pm sized pixels and 3.05 µs pixel dwell time. Laser power detected with these setting is equivalent to using the 'bleachpoint tool', as measured for an pulsed excitation laser (SuperK Extreme EXW-12, NKT Photonics) set at 660 nm wavelength.

Figures

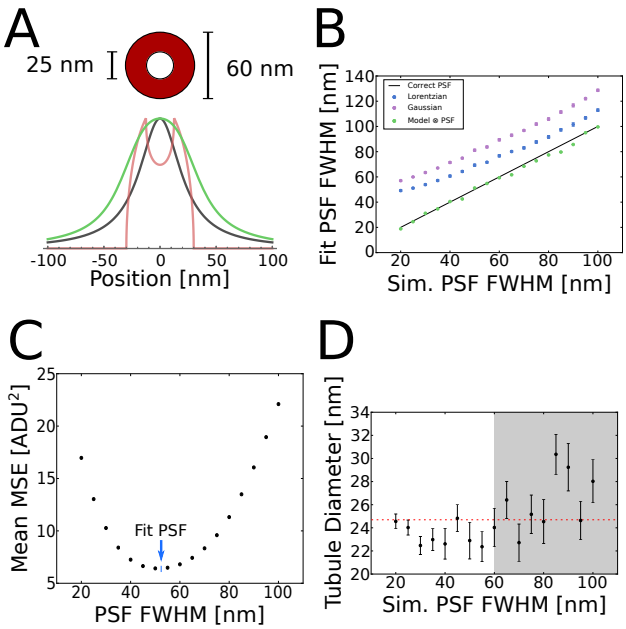

Figure 1: Measuring microscope resolution or sub-cellular features requires advanced fitting techniques. (**A**) Annulus used to model fluorophore location, where antibodies and fluorophores are bound to the 25 nm outer diameter of a microtubule [1], on the surface of the filament. The curves below are relevant to the fitting process. The red curve is a projection of the fluorophore distribution (summing over the axial dimension), and the black curve is a Lorentzian function which models the PSF. The green curve is the antibody-coated tubule model function with the diameter set to that of a microtubule, and is a convolution of the red and black curves. The convolution of the structure projection and PSF is a mathematical operation that occurs physically during imaging. (**B**) Simulated microtubule cross-sections imaged with different resolutions (PSF FWHM), with shot noise added to the profiles, were fit in several ways. Gaussian and Lorentzian fits were applied to the profiles, which shows that the simple Gaussian or Lorentzian fitted FWHM is a rather poor approximation for either the microscope resolution or the structure size (where in this case, the structure is a 25 nm inner diameter, 60 nm outer diameter annulus representing immunofluorescence-labeled microtubules). The same profiles were then fit using NEP fitting with a model function that separately accounts for both the microscope resolution and the fluorophore geometry, which results in good agreement with the ground truth of the simulated microscope resolutions. N=50 profiles were fit for each simulated PSF width. (**C**) Plot of mean MSE of simulated microtubule profiles that were generated with a 50 nm PSF and added shot noise. The fits corresponding to the black points were performed with the same antibody-coated tubule model function we use in NEP fitting, but rather than a minimization function varying the PSF FWHM, the fits were repeated at specified values of the PSF FWHM. NEP fitting seeks to minimize the mean MSE by iteratively fitting the tubule line profile cross sections while varying the PSF width. For microtubules simulated with a 50 nm PSF, the least mean MSE was found to occur when the PSF FWHM is 51.2 nm, as indicated by the blue arrow. (**D**) Plot of NEP fit microtubule diameters, where images were simulated at various resolutions (different PSF FWHM, N=50 profiles at each PSF width, error bars denote standard error of the mean). The inner diameter of the annulus describing the cross section of the fluorophore distribution was 25 nm for all simulated profiles, as shown by the dashed red line. The grey shaded region of the plot indicates where the simulated PSF FWHM is larger than the antibody-coated tubule structure, as the tubule diameter fit is expected to be less accurate in this regime.

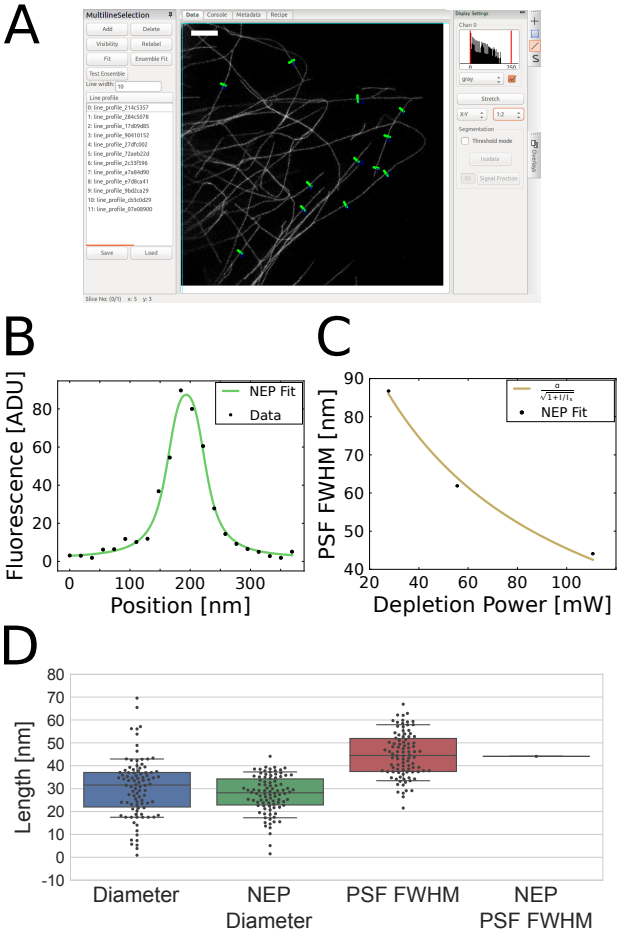

Figure 2: Ensemble PSF Fitting accurately and concomitantly extracts PSF width and tubule diameters of fixed microtubules. (**A**) PYME GUI showing a STED image of immunolabeled microtubules in a COS-7 cell, imaged with 110.6 mW STED power. Green lines show user-selected regions perpendicular to the tubule axis to be used for fitting. (**B**) Plot of raw data from a microtubule profile averaged over 10 pixels along the long axis of the tubule in (*A*) (black points), with accompanying NEP fit (green line). (**C**) Plot of NEP-fit PSF widths from STED images of microtubules acquired with different STED powers (black points), which scales as expected by theory (gold line) (N=74, N=71, and N=94 profiles extracted from n=8, n=8, and n=12 images of n=3, n=3, and n=6 cells, acquired at 27.7, 55.6, and 110.6 mW STED laser powers, respectively). (**D**) Swarm- and box-plots of microtubule diameters and PSF FWHM values determined using NEP fitting, where the PSF is constrained to be the same for all microtubule line profile cross sections, and without NEP fitting, where the PSF is varied separately for each tubule fit. Notably, there is significantly more spread in the microtubule diameters from the fit performed without the constraint that the PSF width is the same for all tubules. The whiskers of boxplots represent the 10th and 90th percentiles of each distribution, the colored boxes cover the interquartile range, and the center line in each box denotes the median.

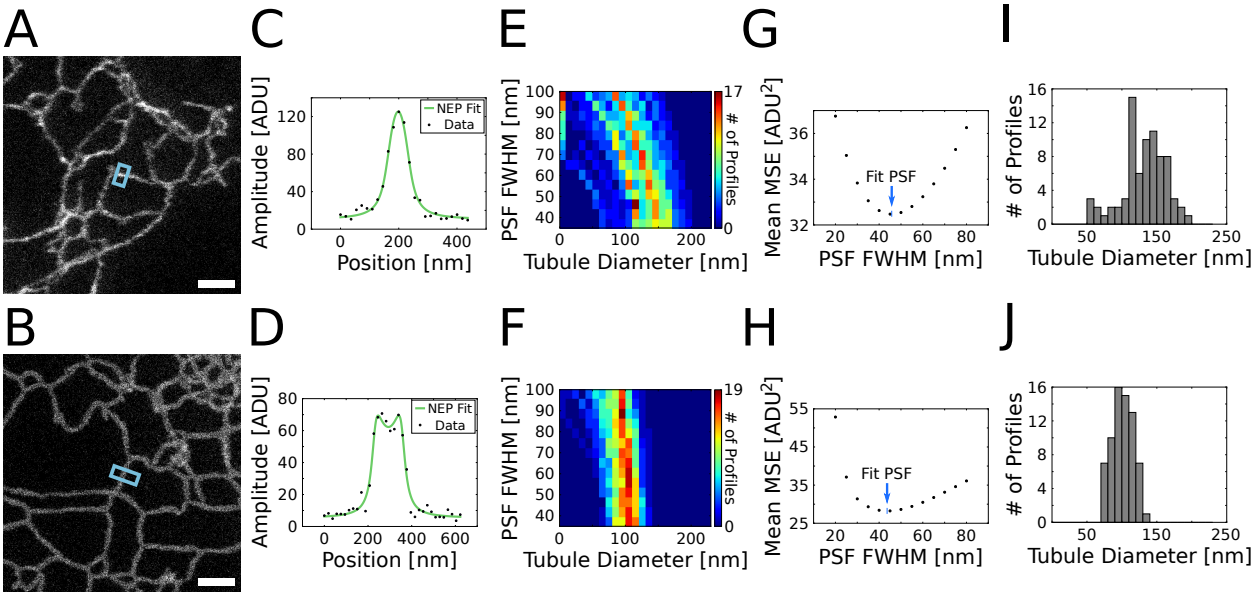

Figure 3: Ensemble PSF Fitting can be applied to images of live-cells, with various labeling schemes. (**A**, **B**) Live-cell STED images of label-filled ((*A*), ss-SNAP-KDEL) and surface-labeled ((*B*), SNAP-sec61β) ER. (**C**, **D**) Fluorescence line profiles, averaged over 10 pixels along the long axis of the tubule, extracted from (*A*) and (*B*) (black points), respectively, and fit using NEP fitting (green line) where the PSF width is constrained to be the same for all line profiles. (**E**, **F**) Heatmaps showing the coupling between tubule diameter and PSF FWHM in non-NEP fitting. Line profiles of ER with label-filled (*E*, ss-SNAP-KDEL) and surface-labeled (*F*, SNAP-sec61β) tubules were fit with the PSF FWHM fixed to a value that was iteratively changed. Intensity corresponds to number of profiles (N=77 and N=69 profiles were extracted from n=7 and n=7 STED images of n=4 and n=2 cells, acquired for ss-SNAP-KDEL and SNAP-sec61β expressing cells, respectively. The images corresponding to each label were acquired on a single day. (**G**, **H**) Mean MSE where the mean is taken over all label-filled (*G*) and surface-labeled (*H*) ER tubule fits when the fits were performed with the PSF FWHM fixed to a value which was iteratively changed. The blue arrow indicates the PSF FWHM found by performing NEP fitting on the same tubule line profiles. (**I**, **J**) Label-filled (*I*) and surface-labeled (*J*) ER tubule diameters fit with the PSF estimated using ensemble PSF fitting (45.8 nm PSF FWHM for ss-SNAP-KDEL, 43.7 nm PSF FWHM for SNAP-sec61β). The mean and standard deviations were 132 $\pm$ 30 nm and 101 $\pm$ 15 nm for ss-SNAP-KDEL and SNAP-sec61β, respectively.

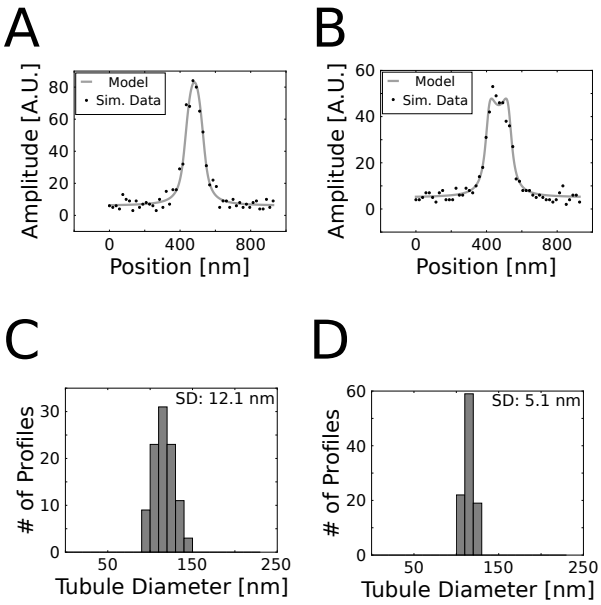

Figure S1: Variance of diameter fits for simulated 115 nm diameter tubules. (**A**, **B**) Plots of simulated profiles of a label-filled (A) and surface-labeled (B) tubule with 115 nm diameter, convolved with a 50 nm FWHM Lorentzian PSF, the expected PSF of our STED microscope. (**C**, **D**) Histograms of fitted tubule diameters for simulated 115 nm diameter label-filled (C) and surface-labeled (D) tubules. NEP fit diameters for the label-filled tubule profiles had a mean of 116 $\pm$ 12 nm (mean $\pm$ SD), and the NEP fit PSF width was 47.5 nm for these profiles. NEP fit diameters for the surface-labeled tubule profiles had a mean of 115 $\pm$ 5 nm (mean $\pm$ SD), and the NEP fit PSF width was 49.3 nm for these profiles. N=100 simulated profiles for both label-filled and surface-labeled models.

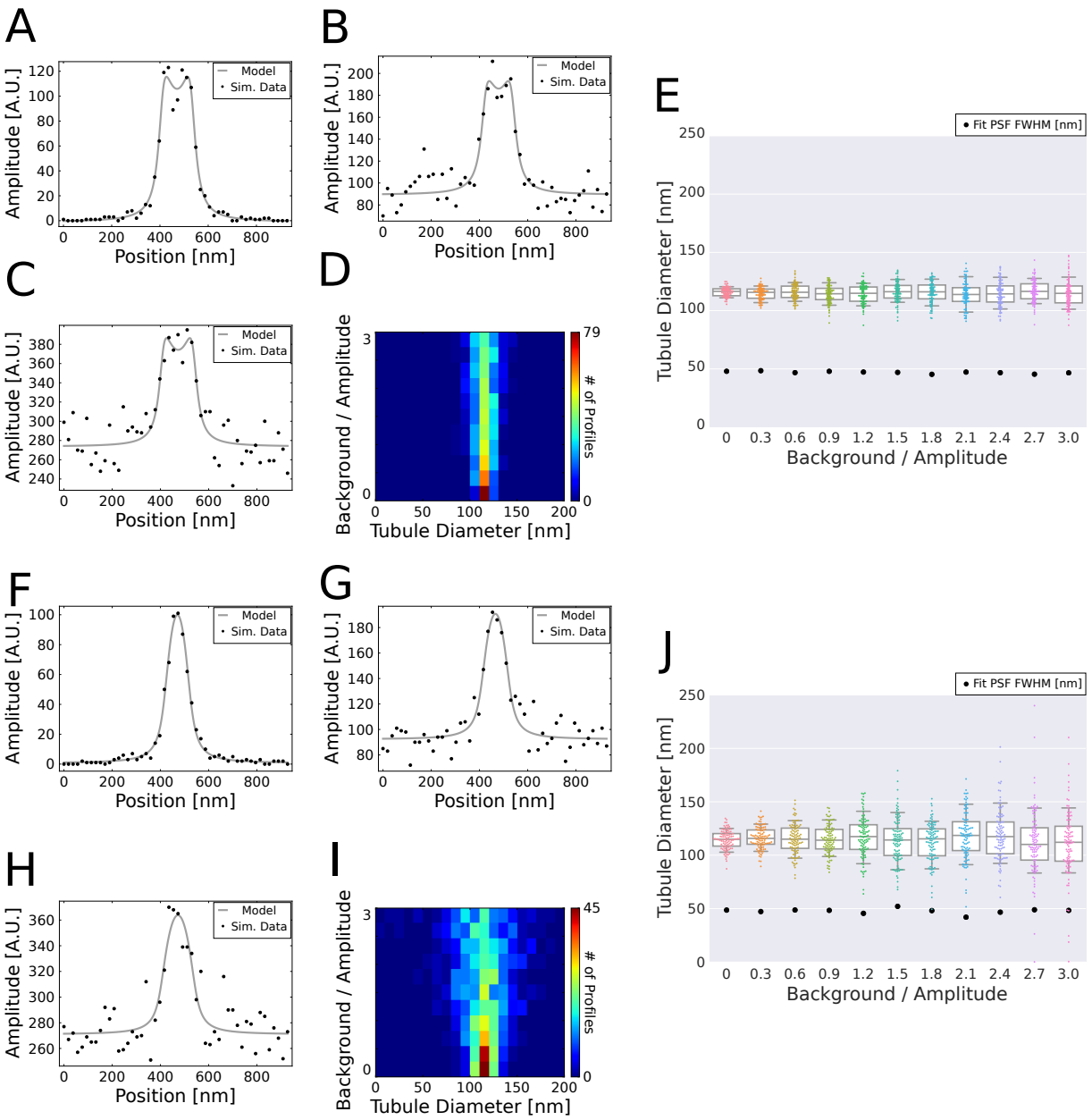

Figure S2: Effect of noise on ER tubule diameter and PSF fitting. (**A**, **B**, **C**) Simulated surface-labeled ER tubules with background to amplitude ratios of 0 (*A*), 0.9 (*B*), and 2.7 (*C*). (**D**) Heatmap of fitted diameters from NEP fits of simulated surface-labeled ER tubule profiles with varied background to amplitude ratios, and therefore varied signal-to-noise ratios. (**E**) Fitted diameters from NEP fits of simulated surface-labeled ER tubules with different background to amplitude ratios. The NEP-fit PSF width is plotted in black. N=100 simulated tubules for each ratio. (**F**, **G**, **H**) Simulated label-filled ER tubules with background to amplitude ratios of 0 (*F*), 0.9 (*G*), and 2.7 (*H*). (**I**) Heatmap of fitted diameters from NEP fits of simulated profiles of label-filled ER tubules with varied background to amplitude ratios, and therefore signal-to-noise ratios. (**J**) Fitted diameters from NEP fits of simulated label-filled ER tubules with different background to amplitude ratios. The NEP-fit PSF width is also plotted in black. N=100 simulated tubules for each ratio. The whiskers of boxplots represent the 10th and 90th percentiles of each distribution, the colored boxes cover the interquartile range, and the center line in each box denotes the median.